Research Article

Rafik El-Mernissi*, Naoual El Menyiy, Rania Moubachir, Aziz Zouhri, Yahya El-Mernissi, Farhan Siddique, Sumaira Nadeem, Hind Ibork, Azeddin El Barnossi, Gezahign Fentahun Wondmie*, Mohammed Bourhia, Yousef A. Bin Jardan, Oualid Abboussi, Lhoussain Hajji

Cannabis sativa L. essential oil: Chemical composition, anti-oxidant, anti-microbial properties, and acute toxicity: *In vitro*, *in vivo*, and *in silico* study

https://doi.org/10.1515/chem-2023-0214
received January 22, 2024; accepted February 14, 2024

Abstract: This study evaluated the volatile components of *Cannabis sativa* L. essential oils (CSEOs) and their pharmacological potential *in vitro*, in animal, and *in silico*. The anti-oxidant capacities of volatile compounds were tested using 2,2-diphenyl-1-picrylhydrazyl (DPPH), ferric reducing antioxidant power (FRAP), total anti-oxidant capacity (TAC), and gas chromatography-mass spectrometry (GC-MS). Anti-microbial activity against bacterial and fungal strains was assessed using disk diffusion and micro-dilution, and acute toxicity was examined on mice using OECD 423 criteria. The results indicate that the main components were β-caryophyllene (31.54%), α-humulene (12.62%), β-myrcene (4.83%), and α-pinene (4.69%). The essential oil showed high anti-oxidant ability (IC_{50} = 0.981 ± 0.059 mg/ml for DPPH, EC_{50} = 1.74 ± 0.05 for FRAP), and TAC of 0.101 ± 0.001 mg AAE/g. Additionally, it showed significant anti-bacterial action against Gram-negative organisms, such as *Escherichia coli* (11.33 ± 0.00 mm), *Klebsiella pneumonia* (9 ± 0.00 mm), and *Pseudomonas aeruginosa* (9.34 ± 0.00), with MICs ranging from 0.0052 to 0.0208 mg/CSEO demonstrated antifungal activity against *Candida albicans* and *Fusarium proliferatum*, with activity levels of 18.66 ± 0.88 mm, 41.89 ± 3.60%, and MICs of 0.39 and 0.013 mg/ml, respectively. In toxicological studies, CSEO proved to be safe for animals. Docking identified bioactive components and explored anti-oxidant and antibacterial properties. Docking proved that bulnesol and champacol caused indicated actions.

Keywords: antimicrobial, antioxidant, *Cannabis sativa* L., essential oils, GC-MS, toxicity

*** Corresponding author: Rafik El-Mernissi**, Bioactives and Environmental Health Laboratory, Faculty of Sciences, Moulay Ismail University, Meknes, B.P. 11201, Morocco; Physiology and Physiopathology Team, Faculty of Sciences, Genomic of Human Pathologies Research Centre, Mohammed V University, Rabat, Morocco, e-mail: ra.elmernissi@edu.umi.ac.ma
*** Corresponding author: Gezahign Fentahun Wondmie**, Department of Biology, Bahir Dar University, P.O. Box 79, Bahir Dar, Ethiopia, e-mail: resercherfent@gmail.com
Naoual El Menyiy: Laboratory of Pharmacology, National Agency for Medicinal and Aromatic Plants, Taounate, 34025, Morocco
Lhoussain Hajji: Bioactives and Environmental Health Laboratory, Faculty of Sciences, Moulay Ismail University, Meknes, B.P. 11201, Morocco, e-mail: l.hajji@umi.ac.ma
Rania Moubachir, Aziz Zouhri: Bioactives and Environmental Health Laboratory, Faculty of Sciences, Moulay Ismail University, Meknes, B.P. 11201, Morocco
Yahya El-Mernissi: Applied Chemistry Research Unit, Faculty of Science and Techniques, Abdelmalek Essaadi University, Al-Hoceima, Tetouan, Morocco
Farhan Siddique: School of Pharmaceutical Science and Technology, Tianjin University, Tianjin, P.R. China
Sumaira Nadeem: Department of Pharmacy, The Women University, Multan, 60800, Pakistan
Hind Ibork, Oualid Abboussi: Physiology and Physiopathology Team, Faculty of Sciences, Genomic of Human Pathologies Research Centre, Mohammed V University, Rabat, Morocco
Azeddin El Barnossi: Biological Engineering Laboratory, Faculty of Sciences and Techniques, Sultan Moulay Slimane University, Beni Mellal, Morocco
Mohammed Bourhia: Laboratory of Biotechnology and Natural Resources Valorization, Faculty of Sciences of Agadir, Ibn Zohr University, Agadir, Morocco
Yousef A. Bin Jardan: Department of Pharmaceutics, College of Pharmacy, King Saud University, P.O. Box 11451, Riyadh, Saudi Arabia

1 Introduction

Folk medicine encompasses medical knowledge systems that have evolved over successive generations [1] From ancient times, people worldwide have been exploring nature in search of remedies to treat their illnesses [2].

Cannabis sativa L. is a plant of the Cannabaceae family and has been utilized for centuries across various domains such as recreation, textiles, religious practice, food, and medicine [3]. Historically, it has been primarily grown and cultivated in Central Asia, particularly in India and China, since ancient times [4]. In Morocco, the cultivation of *Cannabis sativa* L. was banned due to concerns regarding its addictive and psychoactive qualities. However, since 2021 it has become permissible for medicinal and cosmetic uses [5]. In terms of its chemical composition, 565 natural compounds have been identified in *Cannabis sativa* L. [6], including the cannabinoids, flavonoids, terpenes, and alkaloids, that were characterized by important therapeutic benefits such as relief of pain, antiinflammatory [7], antiepileptic and appetite [5–8]. The majority of these elements have not undergone assessment for their pharmacological effects [9].

The emergence of oxidative stress is a key factor in the initiation of numerous chronic diseases. Herbs regarded as a natural reservoir of anti-oxidants, such as polyphenols, terpenoids, and flavonoids, have been identified for their robust anti-oxidant properties, capable of mitigating oxidative stress and thereby preventing the onset of various diseases [2,10]. Presently, the challenges associated with microbial resistance to antibiotics are increasing [11] due to several factors, including the inappropriate use of antibiotics in human health, animal husbandry, and hygiene practices [12]. If no treatment interventions are implemented to control anti-microbial resistance (AMR), it is projected that deaths resulting from AMR infections could reach 10 million by the year 2050 and such a scenario would have a significant and adverse impact on the economy [13]. These global challenges have prompted researchers to find natural products with a wide range of anti-microbial and anti-oxidant properties.

Essential oils (EOs) consist of a mixture of various components that capture the aromatic essence of plants. Around 3,000 EOs have been identified, with approximately 300 holding economic importance, especially in the cosmetic, culinary, and pharmaceutical industries [14]. EOs are recognized for their extensive biological and pharmacological properties, which include antibacterial, antifungal, and anti-oxidant properties [15].

Cannabis areal part contains a variety of terpenes, which are responsible for much of the scent of cannabis, and contribute characteristically to the unique flavor qualities of cannabis products [16]. These lipophilic volatile compounds have the ability to easily cross cellular membranes and the blood–brain barrier, potentially contributing to the pharmacological effects observed in various cannabis preparations [17].

The aerial part of *Cannabis sativa* L. essential oil (CSEO) obtained by hydro-distillation, typically consisting of volatiles and aromatic terpenes, was the subject of few studies in terms of anti-microbial and anti-oxidant activities [18]. Therefore, the purposes of the study were to evaluate the *in vitro* anti-oxidant and anti-microbial activities, pinpoint the specific components within the Moroccan CSEO responsible for these activities, and to study for the first time its safety. Concurrently with *in vitro* and *in vivo* investigation, *in silico* simulations incorporating molecular docking and pharmacokinetic assessments (ADME) were conducted to predict the interactions between molecules identified in gas chromatography-mass spectrometry (GC-MS) analysis and target biomolecules and to assess the various pharmacokinetic characteristics (ADME) of CSEO.

2 Materials and methods

2.1 Plant material

Cannabis sativa L. plant was harvested during the inflorescence stage from the Tafrant region, Taounate, Morocco (34°39′28.4″ N 5°05′58.9″ W), in September 2021. The plant was identified by a botanist at the Scientific Institute of Rabat, and a voucher specimen with the number RAB 112735 was deposited in the Institute herbarium.

2.2 EO distillation

The extraction of air-dried inflorescences and leaves of *cannabis sativa* L. plant was conducted using hydro-distillation in Clevenger-type equipment [19]. In a 2,000 ml flask, a mixture of 150 g of the plant sample and 1,500 ml of distilled water was heated to a boiling point for a duration of 180 min. The obtained EO (CSEO) was dried using anhydrous sodium sulfate and stored in amber glass vials at 4°C. The EO yield was determined by calculating the percentage (v/w) based on the weight of the dried plant material.

2.3 GC-MS analyses

GC-MS analysis of the CSEO was performed using a Thermo Scientific GC system (TRACE GC ULTRA) coupled with a mass spectrometry detector and the split injection method. The GC was fitted with a TG-1MS capillary column (30 m × 0.25 mm: film thickness: 0.25 µm). The temperature program used was as follows: injector temperature, 250°C;

interface line temperature, 250°C; and initial oven temperature, 90°C. The temperature was then programmed to increase at a rate of 1°C per minute until reaching a final temperature of 250°C for 3 min. Helium was employed as the carrier gas at a constant flow rate of 1.5 ml/min. To prepare the EO for injection, 1 µl of the EO was diluted in 1 ml of cyclohexane, and a 1 µl aliquot was automatically injected using an Autosampler Model TriPlus RSH. The electron ionization energy for ionization was set at 70 eV, and the mass range for the analysis was set between 50 and 550 *m*/*z*. The mass spectra of the isolated components were identified based on NIST libraries.

2.4 Anti-oxidant activity

Anti-oxidant defense mechanisms exist in all biological systems to counteract the detrimental effects of oxidative stress. Anti-oxidants are compounds that provide electrons to damaged cells, preventing and stabilizing free radical-induced damage [20].

The anti-oxidant properties of *Cannabis sativa* L. (CSEO) were studied by using three *in vitro* complementary tests: the 2,2-diphenyl-1-picrylhydrazyl (DPPH) free radical scavenging test, total anti-oxidant capacity (TAC), and the reducing power.

2.4.1 DPPH

The study assessed the CSEO capacity to neutralize DPPH radical, employing the approach described by Çapan et al. [21] with slight modification. Briefly, different solutions with varying concentrations, ranging from 10 to 2,000 µg/ml of CSEO, were formulated using ethanol. About 0.1 ml of each test concentration was combined with 0.8 ml of freshly prepared DPPH solution (0.005 g in 200 ml of ethanol absolute). The resultant mixtures were vigorously vortexed and placed in the dark for a 30-min incubation period at room temperature, and the absorbance was recorded at 517 nm using a spectrophotometer (UV-1700APC, China). A blank experiment was conducted following the same procedure, using a solution without CSEO. The scavenging (%) of DPPH free radical by CSEO was calculated using the following formula:

$$\%\text{Scavenging DPPH} = \frac{(\text{Control absorbance} - \text{Samples absorbance})}{\text{Control absorbance}} \times 100$$

IC_{50} values were calculated graphically, and butylated hydroxytoluene (BHT) and quercetin prepared under the same conditions and concentrations were utilized as reference substances for comparison. The examination was repeated three times.

2.4.2 TAC

The TAC was determined using the phosphomolybdate technique outlined in a prior investigation [22]. The concentration of TAC was assessed using the equation derived from the standard ascorbic acid curve, and the findings are presented in milligrams of ascorbic acid equivalents per gram of EO (mg AAE/g of EO). The experiment was conducted thrice.

2.4.3 Reducing power

The reductive capability of CSEO was assessed following the method described earlier [23]. In brief, a stock solution of CSEO (2,000 µg/ml) was prepared in absolute ethanol. A series of dilutions was created, resulting in ten consecutive dilutions (10–2,000 µg/ml), and 100 µl of each concentration was added to 200 µl of sodium phosphate buffer (0.2 M; pH = 6.6) and 200 µl of potassium ferricyanide (1%). After 20 min of incubation at 50°C, 200 µl of distilled water, 120 µl of 0.1 % ferric chloride, and 200 µl of trichloroacetic acid (10%) were added. The absorbance was determined at 700 nm. The test was replicated three times, with BHT and quercetin serving as positive controls prepared under the same conditions with the same used concentrations (10–2,000 µg/ml), and the EC_{50} values were estimated graphically.

2.5 Anti-microbial activity of CSEO

2.5.1 Microbial strains

The anti-microbial effectiveness of CSEO was evaluated against four types of fungi (*Candida albicans*, *Aspergillus niger*, *Aspergillus flavus*, and *Fusarium proliferatum*) and four bacterial strains (*Staphylococcus aureus*, *Escherichia coli*, *Klebsiella pneumonia*, and *Pseudomonas aeruginosa*) (Table 1).

2.5.2 Antibacterial activity

The assessment of the antibacterial activity of CSEO was carried out through the disk diffusion technique [24].

Table 1: List of microbial strains examined

Bacterial strains	Code
Staphylococcus aureus	ATCC6633
Escherichia coli	K12
Klebsiella pneumoniae	CIP A22
Pseudomonas aeruginosa	CIP 82.114
Fungal strains	
Candida albicans	ATCC 10231
Aspergillus niger	MTCC282
Aspergillus flavus	MTCC9606
Fusarium proliferatum	MTCC 9913

Indeed, culture plates containing Mueller–Hinton (MH) culture medium were individually infected with the four tested bacterial strains using the double-layer approach. Starting from fresh cultures of each bacterium, decimal dilutions were created in sterile saline solution (0.9% NaCl) until a turbidity of 0.5 McFarland (106–108 CFU/ml) was attained. Subsequently, 100 µl of each bacterial culture was added to separate tubes containing 5 ml of soft agar (0.5% agar–agar in MH medium). The tubes containing the inoculated mixture were poured into Petri dishes containing the MH medium. Sterile discs of Whatman paper (6 mm in diameter) were placed at the central region of the inoculated Petri dish and soaked in 20 µl of CSEO. Positive controls were prepared following the identical steps, employing the antibiotic cephalothin (30 µg/disc). The Petri dishes with inoculated samples were incubated at 37°C, in darkness, and in a moisture-saturated environment. The inhibition diameter was determined after 24 h of incubation [25].

2.5.3 Antifungal activity

The evaluation test for the antifungal activity of CSEO was also conducted using the disk diffusion assay [24]. In the case of *C. albicans,* we followed the same principles and protocols that were used to assess the antibacterial activity. However, for filamentous fungi, the antifungal activity evaluation was performed on Malt Extract agar medium but through confrontation between each harmful fungus and 20 µl of oil, according to Pereira et al. [26]. Positive controls were carried out following the same steps and using the antifungal antibiotic Fluconazole (15 mg/ml). The inoculated Petri dishes were incubated in the dark and under a humidity-saturated atmosphere at 37°C and 30°C for *C. albicans* and harmful molds, respectively. The measurement of the inhibition zone (IZ) diameter and determination of the inhibition rate were performed after 48 h of incubation for *C. albicans* and after 7 days of incubation for harmful molds, respectively [25,27].

2.5.4 Determination of the minimum inhibitory concentration (MIC)

The microdilution method, as described by Sarker et al. [28], was employed to determine the MICs of CSEO against the four bacterial and four fungal strains. In summary, a microdilution process involved serially diluting the sample by a factor of 2 in each well, with the exception of the final well, which served as a positive control for growth. Following respective incubation periods of 24 h for bacteria, 48 h for *C. albicans*, and 7 days for *A. niger, A. flavus*, and *F. proliferatum* at temperatures of 37°C and 30°C. MIC was determined using the colorimetric method involving 0.2% (w/v) 2,3,5-triphenyltetrazolium chloride [29].

2.6 Acute oral toxicity study

The Organization of Economic Cooperation and Development Standards (OECD 423) were used to assess the acute toxicity of CSEO [30]. Twenty-four male and female mice (20–24 g) were supplied by the Faculty of Sciences Moulay Ismail Meknes. They were randomly subdivided into two groups, and each group consisted of 12 animals with an equal distribution of six males and six females in each group. After fasting overnight, the tested group received CSEO by oral route at a single dosage of 2 g per kilogram of body weight, and the control group received distilled water. The groups had unrestricted access to both food and water. Body weight changes and general behavior were monitored daily for a duration of 14 days. On the 15th day, all the rats underwent a 16-h fasting period before being euthanized for necropsy examination. The heart, liver, kidneys, and spleen weights were measured in proportion to the final body weight. Additionally, thorough visual inspections were conducted to observe any visible abnormalities in the tissues.

2.7 Molecular docking studies

CSEO was examined through GC-MS, and its antibacterial potential and anti-oxidant properties were assessed using Schrodinger Glide software through docking analysis [31]. The three-dimensional structures of all the proteins, such as crystal structure of bovine xanthine oxidase in complex with hypoxanthine (PDB ID: 3NRZ, resolution 1.7 Å), crystal

structure of Staph GyraseB 24 kDa in complex with Novobiocin (PDB ID: 4URO, resolution 2.59 Å), were used for the molecular modeling and were retrieved from the website of Protein Data Bank (http://www.rcsb.org/pdb/home/home) [32]. The ligands being analyzed were examined for their theoretical binding mode to observe potential intermolecular interactions with the receptor. The necessary protein structures were preprocessed, optimized, and minimized using the Protein Preparation Wizard within the Schrödinger software's graphical interface, Maestro v12.8. Water molecules identified through crystallography and forming one or two hydrogen bonds were eliminated. Additionally, to adjust the protein's pH to 7.0, hydrogen atoms were incorporated into the structure. Restrained minimization of the heavy atoms was conducted to achieve an RMSD cutoff of 0.30 Å. The ligands (dataset) underwent preparation utilizing the LigPrep module within Schrödinger v12.8. A radius of 20 Å was used to define the active site around the ligand within the crystal structure of the proteins. In addition, a grid box was created surrounding the centroid of the specified active site. The ligands (including the co-crystallized ligand), along with their low-energy conformations, were docked into the catalytic pockets of the selected anti-oxidant and antibacterial target proteins. Structures demonstrating the most favorable outcomes were chosen according to their docking scores and binding energies.

2.8 ADME study *in silico*

The pharmacokinetic and pharmacodynamics properties of EOs of *Cannabis sativa* L. were determined by employing a freely available online software SwissADME tool.

2.9 Statistical analyses

The mean values, along with their corresponding standard deviations, were computed utilizing GraphPad Prism 9.5 software. The obtained results were subjected to comparison through a two-way ANOVA, followed by the Tukey test as a post-hoc analysis. Any variance with a significance level of $p < 0.05$ was deemed as a meaningful difference.

3 Results and discussion

3.1 EO yield

The yield of CSEO was 0.14 ± 0.03 % v/w, which aligns with findings documented in the existing literature [33–35] and is lower than those obtained in previous studies [19,36–41]. CSEO yields exhibit significant variability, influenced by a diverse array of factors, such as cultivar variety, drying techniques, duration of extraction, choice of solvent, extraction methodology, harvesting period, and the specific plant part utilized for extraction, as cited in earlier studies [42–44].

3.2 GC-MS analyses

The examination of the volatile composition of CSEO through GC-MS analysis revealed the presence of 24 sesquiterpenes (75.68%), 7 monoterpenes (17.08%), and the absence of cannabinoids. Out of the total identified terpenes, 22 had concentrations exceeding 1%, while the remaining 9 terpenes were found in concentrations below 1% (Table 2, Figure 1). As previously reported, sesquiterpenes and monoterpenes were identified as the main constituents of the EO of the majority of plants [45].

Among the sesquiterpenes, β-caryophyllene was found to be the dominant component, constituting 31.54% of the composition, followed by α-humulene (12.62%), elina-3,7(11)-diene (3.36%), aromadendrene (2.94%), and caryophyllene oxide (2.46%). In contrast, bulnesol was present as the minor compound, making up only 0.54% of the total composition. Additionally, it was noted that β-myrcene (4.83%), α-pinene (4.69%), and D-limonene (3.10%) were the dominant monoterpenes in the CSEO.

Our results are consistent with earlier studies in the literature concerning the EOs derived from various *Cannabis sativa* L. cultivars from Morocco and other countries, and *β*-caryophyllene consistently stands out as the predominant constituent [40,41]. This result is based on the study of Novak et al. [46] and Kumeroa et al. [47], while other works show the presence of cannabinoids as a minor constituent in CSEO [41,44,45]. Compared with the results obtained by El Bakali et al. [19] and Nafis et al. [44], we worked on the same cultivar of cannabis, and some differences in compositions were observed, such as the presence and absence of some minor constituents and the percentage of others. These can be explained by the geographic provenances of the plants, as concluded previously [48].

3.3 Anti-oxidant activity

As the anti-oxidant activity should not rely solely on one anti-oxidant test model [49], in practice, it is advisable to conduct multiple *in vitro* tests to investigate the anti-

Table 2: Chemical composition of the CSEO

Retention time	Compounds	Cas n	Chemical structure	Chemical nature	Area %
7.77	α-Pinene	80-56-8	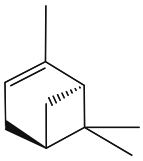	Monoterpene	4.69
9.42	β-Pinene	127-91-3	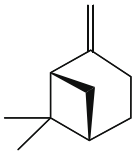	Monoterpene	1.34
9.96	β-Myrcene	123-35-3	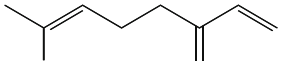	Monoterpene	4.83
11.40	D-Limonene	5989-27-5	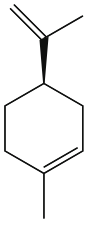	Monoterpene	3.10
11.71	Eucalyptol	470-82-6	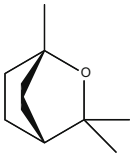	Monoterpene	0.83
12.11	β-OCIMENE	13877-91-3	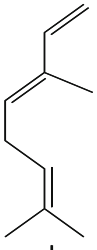	Monoterpene	0.76
18.11	α-Terpineol	10482-56-1	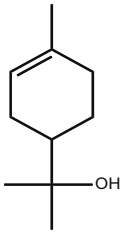	Monoterpene	1.53
22	Nd	—	—	—	2.19
24.35	γ-Caryophyllene	118-65-0	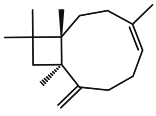	Sesquiterpene	1.27
24.95	β-Caryophyllene	87-44-5	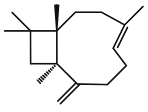	Sesquiterpene	31.54
25.23	α-*trans*-Bergamotene	17699-05-7	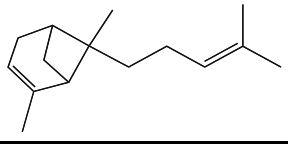	Sesquiterpene	2.41

(Continued)

Table 2: *Continued*

Retention time	Compounds	Cas n	Chemical structure	Chemical nature	Area %
25.90	(*E*)-β-Farnesene	18794-84-8	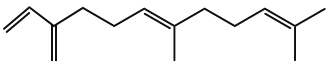	Sesquiterpene	1.90
26.06	*α*-Humulene	6753-98-6	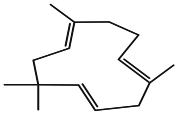	Sesquiterpene	12.62
26.15	9-epi-β-Caryophyllene	68832-35-9	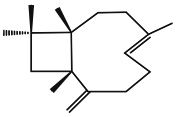	Sesquiterpene	1.36
27.07	(−)-β-Selinene	17066-67-0	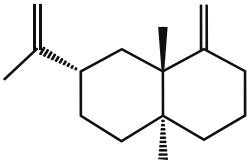	Sesquiterpene	1.36
27.27	α-Guaiene	3691-12-1	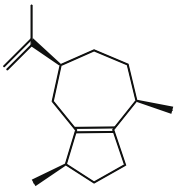	Sesquiterpene	1.34
27.40	δ-Guaiene	3691-11-0	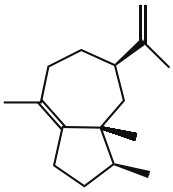	Sesquiterpene	0.81
27.49	α-Farnesene	502-61-4	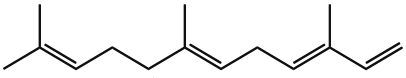	Sesquiterpene	0.84
27.59	β-Bisabolene	495-61-4	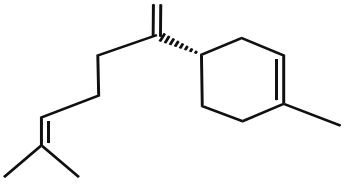	Sesquiterpene	0.77
27.93	γ-Gurjunene	22567-17-5	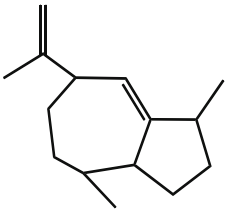	Sesquiterpene	0.76
27.93	β-Maaliene	36577-33-0	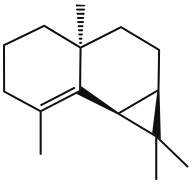	Sesquiterpene	0.87
28.53	Aromadendrene	489-39-4	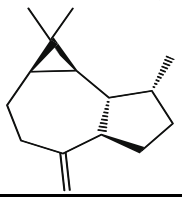	Sesquiterpene	2.94

(Continued)

Table 2: *Continued*

Retention time	Compounds	Cas n	Chemical structure	Chemical nature	Area %
28.57	(*E*)-α-Bisabolene	25532-79-0	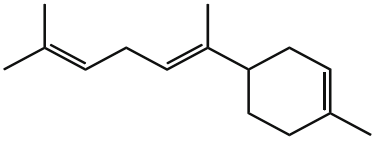	Sesquiterpene	1.41
28.64	Selina-3,7(11)-diene	6813-21-4	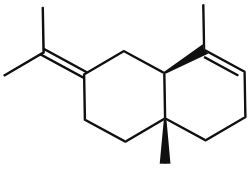	Sesquiterpene	3.36
29.38	*E*-Nerolidol	40716-66-3	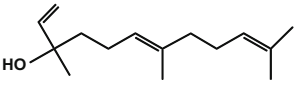	Sesquiterpene	0.85
30.07	Caryophyllene oxide	1139-30-6	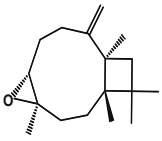	Sesquiterpene	2.46
30.54	Champacol	13822-35-0	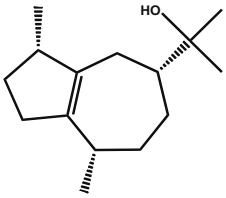	Sesquiterpene	1.74
30.90	Humulene oxide II	19888-34-7	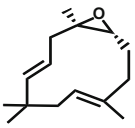	Sesquiterpene	1.02
31.25	γ-Eudesmol	1209-71-8	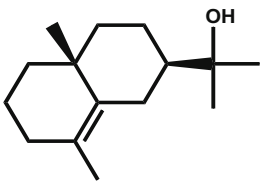	Sesquiterpene	1.08
31.68	β-Eudesmol	473-15-4	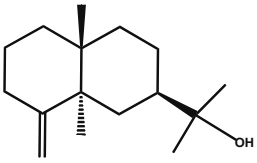	Sesquiterpene	2.07
32.48	Bulnesol	22451-73-6	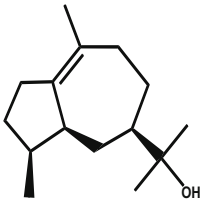	Sesquiterpene	0.54
33.01	α-Bisabolol	515-69-5	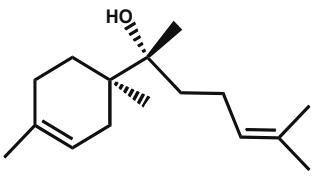	Sesquiterpene	1.72
35.66	Nd	—	—	—	1.22
40.49	Nd	—	—	—	0.81

(Continued)

Table 2: *Continued*

Retention time	Compounds	Cas n	Chemical structure	Chemical nature	Area %
Monoterpenes				17.08	
Sesquiterpene				75.68	
Nd				4.22	
Total area				96.98	

Nd: not determined.

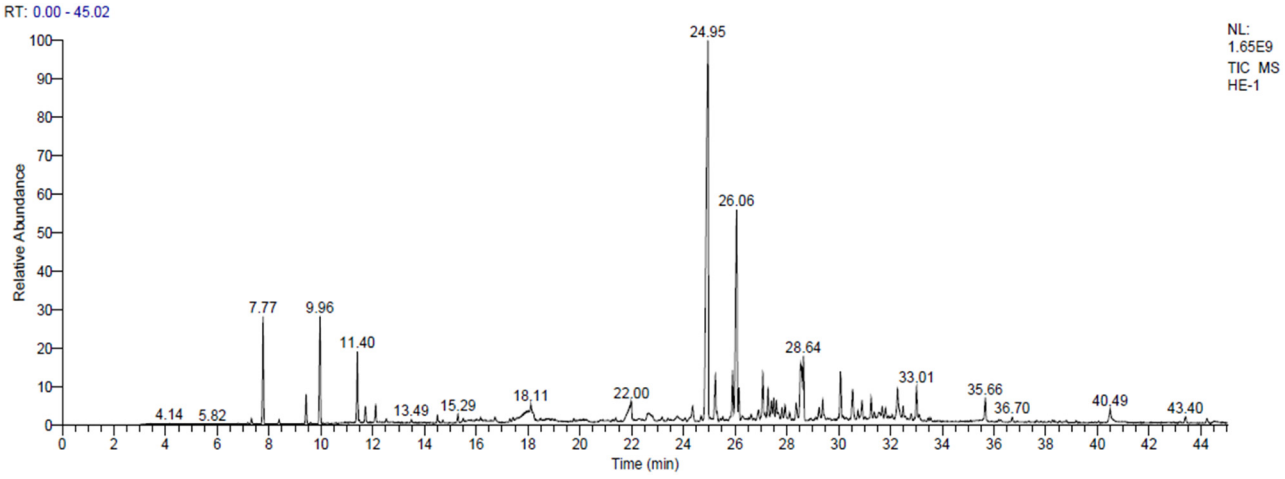

Figure 1: GC-MS chromatogram of CSEO.

oxidant potential of the samples under investigation [49]. In this respect, three complementary colorimetric tests were used, and the results are presented in Table 3.

DPPH is frequently employed as a reactive hydrogen acceptor to evaluate the ability of diverse anti-oxidant compounds derived from medicinal plants. The concentration of CSEO required to scavenge 50% of DPPH was 0.981 ± 0.059 mg/ml. This value is higher than that of BHT (0.0141 ± 0.001 mg/ml) and quercetin (0.120 ± 0.003 mg/ml).

The results of the ferric reducing antioxidant power (FRAP) test revealed the ability of the CSEO to convert Fe^{3+} into Fe^{2+} with an EC_{50} value of 1.74 ± 0.05 mg/ml. However, it is important to note that this reducing capability was markedly less potent than the synthetic standards, BHT (EC_{50} = 0.0141 ± 0.001 mg/ml) and quercetin (0.120 ± 0.003 mg/ml).

The results of the TAC test indicated that the TAC of CSEO, as well as the standards BHT and quercetin, were 0.101 ± 0.001 mg AAE/g EO, 0.055 ± 0.003 mg AAE/g EO, and 0.037 ± 0.002 mg AAE/g EO, respectively.

The results of the anti-oxidant test reveal interesting anti-oxidant properties, which may be attributed to varying chemical compounds found in the oil, particularly the relatively elevated percentages of β-caryophyllene and α-humulene, known for their antioxidative activities [50,51], while it is possible that other compounds like β-myrcene, α-pinene, aromadendrene, and D-limonene could be involved with the synergistic effect [52,53]. It is noteworthy that the results of anti-oxidant effects are similar to those reported by Nafis et al. [44]. Moreover, they were higher than those found in other research studies on industrial cannabis cultivars (Kompolti, Carmagnola Lemon, Carmagnola, Futura 75, Gran Sasso Kush) [54,55] and lower than those in carmagnole, selezionata, and eletta campana cultivars investigated

Table 3: Anti-oxidant activities of CSEO

	DPPH (IC_{50} mg/ml)	FRAP (EC_{50} mg/ml)	TAC (mg AAE/g EO)
CSEO	0.981 ± 0.059[a]	1.74 ± 0.05[a]	0.101 ± 0.001[a]
BHT	0.0141 ± 0.001[b]	0.030 ± 0.003[b]	0.055 ± 0.003[b]
Quercetin	0.120 ± 0.003[c]	0.022 ± 0.001[c]	0.037 ± 0.002[b]

Mean ± SD in the same row followed by different letters (a,b,c) are statistically significant, n = 3.

by Menghini et al. [40]. These findings provide a foundation for future investigations that may pave the way for CSEO as a natural anti-oxidant agent in pharmaceutical applications.

3.4 Anti-microbial activity of CSEO

3.4.1 Antibacterial activity

The anti-microbial properties of CSEO were assessed by determining their IZ diameters and the MICs. As illustrated in Table 4, *E. coli* and *K. pneumonia* were resistant to cephalothin, and CSEO was noted to be active against all bacteria strains tested, except *S. aureus*. The IZ and MIC values of the EOs were significantly lower compared to those of cephalothin. *K. pneumonia* was the least sensitive strain with an IZ of 9 mm and an MIC of 0.0104 mg/ml, followed by *P. aeruginosa* (IZ = 9.34 mm, MIC = 0.0208 mg/ml) and *E. coli* (IZ = 11.33 mm, MIC = 0.0052 mg/ml).

The antibacterial activity of EO from industrial cannabis is well documented in the literature [56–58]. However, researchers have paid minimal attention to studying the cannabis drug types [29]. Nissen and coworkers evaluated the anti-microbial activity of EOs derived from the flowers of three distinct varieties of *C. sativa* L., and single terpenes standards. The entirety of the EOs, especially the Futura variety, displayed notable effectiveness against microbial strains. The terpene standard, α-pinene, showed the highest efficacy against both Gram-positive and Gram-negative bacteria [18]. In recent research, Iseppi et al. detailed the chemical composition analysis of 17 CSEOs and their antibacterial potential besides the effect of pure compounds, such as β-caryophyllene, β-pinene, α-pinene, β-myrcene, α-terpinolene, and cannabidiol. The findings indicated significant antibacterial activity of six hemp EOs in a strain-dependent manner, as in our case, among the pure compounds tested, β-myrcene, β-pinene, α-pinene, and cannabidiol, demonstrated significant antibacterial activity [59]. Earlier research proposed that terpenes from EO may exert their anti-microbial effects by disrupting the cell membrane [60], and the moderate antibacterial potency of CSEO may be related to the high content of β-caryophyllene and α-humulene potentially effective against bacterial infections [61–63], and its terpene profile rich of α-pinene, β-pinene, and β-myrcene [64,65]. The major and minor compounds of CSEO may have individual or synergistic effects [44,59].

3.4.2 Antifungal activity

Fungal infections, caused by real-nucleus organisms, present a greater challenge in both identifying their presence and administering suitable therapeutic remedies when compared to bacterial infections [66]. EOs have emerged as among the most auspicious natural products for inhibiting fungal growth. Typically, the active anti-microbial compounds found in EOs are terpenes, characterized by a high lipophilic nature and relatively low molecular weight demonstrating inefficiency as anti-microbial agents [67,68]. Moreover, complete EOs exhibit heightened antifungal activity, potentially due to certain synergistic or antagonistic effects between terpenic components [68,69]. Numerous research works have presented intriguing findings regarding the functional mechanisms of EOs against fungi, such as cell membrane disruption, dysfunction of the fungal mitochondria, inhibition of efflux pumps, and ROS production [70], although it is still not fully understood [67].

The antifungal assay results indicate that the CSEO was ineffective against *A. niger* and *A. flavus*. The CSEO was less pronounced than the standard reference fluconazol. For the other strain, *F. proliferatum* showed the highest susceptibility to CSEO, with an inhibition percentage of 41.89 ± 3.60%. On the other hand, *C. albicans* exhibited lower sensitivity to CSEO, with an inhibition percentage of 28.51 ± 0.69%. The microdilution assay showed that the lowest MIC was recorded for *F. proliferatum* (0.013 mg/ml), while *C. albicans* exhibited a higher MIC value (0.39 ± mg/ml).

Table 4: Antibacterial activities and MICs of CSEO and the standard (cephalothin)

	Cephalothin		CSEO	
	IZ diameters (mm)	**MIC (mg/ml)**	**IZ diameters (mm)**	**MIC (mg/ml)**
S. aureus	28 ± 0.00	0.00156 ± 0.00	0	—
E. coli	0	—	11.33 ± 0.00	0.0052 ± 0.00
K. pneumonia	0	—	9 ± 0.00	0.0104 ± 0.00
P. aeruginosa	15 ± 0.00[a]	0.00156 ± 0.00[a]	9.34 ± 0.00[b]	0.0208 ± 0.00[b]

Mean ± SD in the same row followed by a different letter (a,b) are statistically significant, $n = 3$; MIC: minimum inhibitory concentration; (−): resistant.

In contrast, bioactive constituents of CSEO, including β-caryophyllene and its isomer, α-pinene, β-pinene, β-myrcene, and champacol, might be behind the moderate fungicidal action [61,67,69,71,72].

The outcomes of the antifungal assay support the report of some earlier papers. Wanas et al. reported that the volatile oil *Cannabis sativa* L. displayed a modest antifungal potential as well as its three fractions characterized by α-humulene, β-caryophyllene, and caryophyllene oxide [57]. A recent study by Nafis and coworkers showed that four *Candida* strains were mildly susceptible to CSEO with a similar MIC of 9.5 mg/ml [44]. Similar results were observed by Nissen et al., who evaluated the anti-microbial effectiveness of three legal hemp EOs on yeast [18]. Moreover, Zengin et al. reported that the EO of hemp was ineffective against yeasts [41]. Likewise, the findings of Ali and his team revealed that the oil of the cannabis seeds, the extract obtained from the entire plant using petroleum ether, and the methanol extract of the whole plant were inactive against *A. niger* [73]

Conversely, EOs of four *Cannabis sativa* L. from three industrial hemp varieties from Italy showed strong mycostatic effects toward dermatophyte strains [74]. Additionally, the ethanolic extract of *Cannabis sativa* L. resins demonstrates potent anti-yeast against *S. cerevisiae*, besides a marked fungistatic activity counter *F. eumartii*, by the inhibition of hyphae elongation and spore germination [75].

Most likely, the CSEO has a selective activity against fungi. Continued investigation within this field may uncover novel perspectives and contribute to the development of sustainable and effective methods for managing fungal diseases (Table 5).

3.5 Acute oral toxicity study

Examining toxicity is crucial in extensive investigations of potential medicinal substances. It not only gauges the safety of the drug but also establishes the maximum doses for therapies without harmful effects [76]. Despite the pharmacological advantages and cosmetic potentials attributed to CSEO [77], there is a lack of comprehensive information regarding the toxicity profile of this EO, and for this reason, it is essential to determine its safety profile as a fundamental guideline for its usage.

Oral administration was primarily chosen due to the absence of a standardized inhalation procedure specifically designed for mice. Administering CSEO orally at a dosage of 2 g/kg showed no fatalities or signs of toxicity (diarrhea, sedation, urination, change in skin, alteration in food and water consumption, or locomotor activity). Therefore, it can be inferred that CSEO is virtually nontoxic in acute administration. This finding indicates that the lethal dose 50 (LD_{50}) might be higher than 2 g/kg. This result aligns with that of Balafrej et al. [78]; on the contrary, Yassa et al.'s study on male rats revealed an LD_{50} of 1729.6 mg/kg. In essence, within an acute toxicity study, the dosage of a plant extract is typically regarded as toxic if it leads to a decrease in body weight of 10% or more in the treated animals [79]. It is crucial to highlight that throughout the 14-day acute oral toxicity investigation, the findings presented in Figure 2 and Table 6 demonstrate that there were no significant changes in body or relative organ weights of both genders when compared to the control groups. This outcome indicated that the CSEO had no impact on the increase of body weight in mice. Moreover, upon visual examination, the internal organs of all the mice showed no observable abnormalities. These outcomes are consistent with those of earlier research [78,80,81]; on the other hand, unlike our study, these previous findings indicated signs of toxicity like reduced activity and somnolence, potentially attributed to the sedative influence of cannabinoids [82].

3.6 Glide molecular docking studies

With the view to elucidate the mode of interaction of active compounds with the anti-oxidant and antibacterial

Table 5: Antifungal activities and MICs of CSEO and standard (fluconazol)

	Fluconazole (15 mg/ml)		CSEO	
	IZ diameters	**MIC (mg/ml)**	**IZ diameters**	**MIC (mg/ml)**
C. albicans	41.33 ± 1.15^{a} mm	0.0117	18.66 ± 0.88^{b} mm	0.39
A. niger	47.67 ± 1.59%	0.586	0	—
A. flavus	43.67 ± 1.53%	0.117	0	—
FFusarium proliferatum	59.17 ± 0.76^{a}%	0.586	41.89 ± 3.60^{b}%	0.013

Mean ± SD in the same row followed by different letters are statistically significant, n = 3; MIC: minimum inhibitory concentration; (−): resistant.

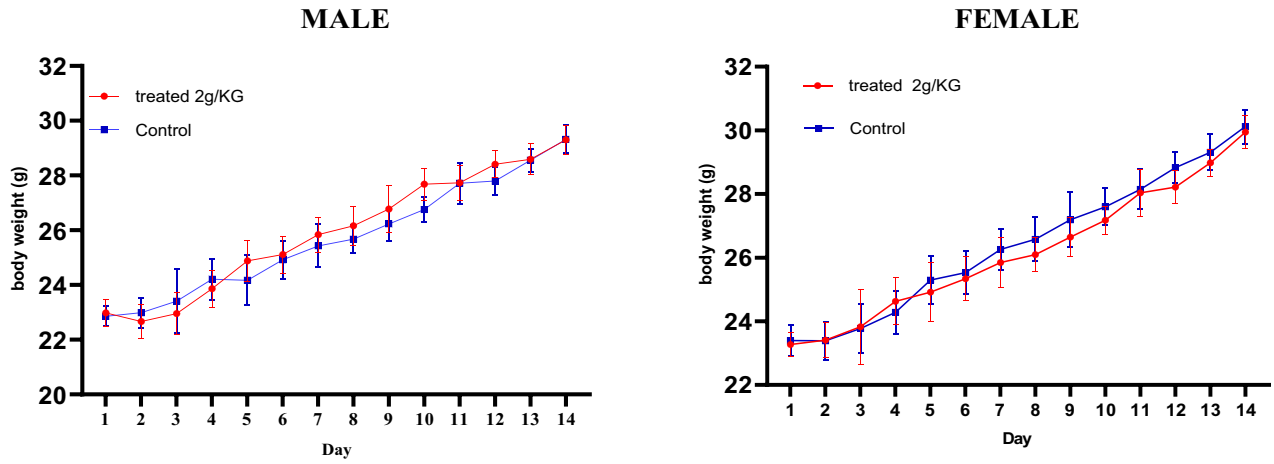

Figure 2: Body weight changes in male and female mice treated orally with a single dose of CSEO 2 g/kg, in 14 days; the values are expressed as mean ± SD.

Table 6: Relative organ weights of male and female mice treated orally with a single dose of CSEO 2 g/kg, *n* = 5 mice/group

	Groups			
	Male		Female	
	Treated	Control	Treated	Control
Heart	0.38 ± 0.02	0.35 ± 0.02	0.35 ± 0.03	0.40 ± 0.03
Liver	4.35 ± 0.08	4.30 ± 0.29	3.85 ± 0.42	3.84 ± 0.38
Kidney	0.65 ± 0.04	0.70 ± 0.11	0.40 ± 0.07	0.34 ± 0.06
Spleen	0.95 ± 0.05	0.91 ± 0.07	0.92 ± 0.06	0.81 ± 0.07

There was no significant difference in relative organ weights of male and female mice when compared to control groups; the values are expressed as mean ± SD.

activities, the GLIDE module was used to carry out the molecular docking study, and the findings were examined based on glide energy and docking scores and are presented in Table 7. The obtained docking poses were examined visually, and the interactions of the molecules with the residues of the binding pocket were comprehended with the help of ligand interactions (3D and 2D) diagrams. The docking scores are presented in terms of negative values; the lower the docking score and glide energy, the better the binding affinity. It was concluded that the majority of the active compounds showed high glide docking scores against the selected target proteins under investigation.

In the case of the anti-oxidant target protein (PDB ID: 3NRZ), bulnesol, the glide docking and their corresponding binding energies (−8.013, −47.856 kcal mol^{-1}) were observed to be the highest among the extracted EOs, followed by champacol (−7.645, −47.716 kcal mol^{-1}) as compared to those of the co-crystallized ligand (−10.375, −90.026 kcal mol^{-1}).

The co-crystallized ligand of anti-oxidant target protein yielded a glide docking score of −10.375 kcal/mol, engaging in hydrogen bonding with LYS249 (1.96 Å), PRO253 (1.78 Å), GLU254 (2.23 Å), LYS256 (2.72 Å), ARG394 (2.07 Å), and THR396 (1.93 Å, 5.33 Å) at their respective distances mentioned in parentheses. The amino acid residues ILE19, VAL27, LEU152, and ALA162 show hydrophobic interactions. ASN261, SER347, THR354, and THR396 are accountable for polarity. This can be seen in Figure 3. PRO253, ALA255, LEU257, VA258, VAL259, ILE264, PHE275, PRO281, LEU287, ALA301, ALA302, ILE353, LEU398, PRO400, ILE403, and LEU404 are hydrophobically involved amino acids.

Figure 4 is the visual display of bulnesol interaction with the anti-oxidant target receptor 3NRZ. Bulnesol shows a glide docking score of −8.013 kcal/mol and forms hydrogen bonding interactions with LEU257 at a distance of 1.90 Å. LEU257, VA258, VAL259, ILE264, LEU287, ALA301, ALA302, ILE353, LEU398, ILE403, and LEU404 are hydrophobically involved amino acids, whereas SER347 and THR354 are polar amino acids.

Figure 5 is the pictorial display of champacol interaction with the anti-oxidant target receptor 3NRZ. It shows a glide score of −7.645 kcal/mol and no hydrogen bonding is evident. LEU257, VA258, VAL259, ILE264, PRO281, LEU287, ALA301, ALA302, ALA346, ILE353, and LEU404 are hydrophobically involved amino acids. The polar amino acid residues are ASN261, THR262, SER347, and THR354.

For the receptor 4URO (antibacterial target protein), the co-crystallized ligand as shown in Figure 6, exhibits a prominent glide score of −5.904 kcal/mol, showing hydrogen bonding interactions with amino acids ASN54 (2.12 Å), GLU58 (2.35 Å), ASP81 (2.08 Å), GLY85 (2.53 Å), and GLN91 (1.97 Å). The hydrophobic interactions are visible with ILE51, VAL79, ILE86, PRO87, ALA98, VAL101, ILE102, and

Table 7: Glide molecular docking data of hit bioactive constituents investigated for anti-oxidant and antibacterial activities

Ligands	Docking score (kcal/mol)	Glide score (kcal/mol)	Glide model (kcal/mol)	H-bonding and distance (Å)	Polar amino acid residues	Hydrophobic interactions
3NRZ (anti-oxidant)						
(a) Co-crystallized ligand-3NRZ (anti-oxidant)	−8.288	−10.375	−90.026	LYS249 (1.96), PRO253 (1.78), GLU254 (2.23), LYS256 (2.72), ARG394 (2.07), THR396 (1.93, 5.33)	ASN261, SER347, THR354, THR396	PRO253, ALA255, LEU257, VA258, VAL259, ILE264, PHE275, PRO281, LEU287, ALA301, ALA302, ILE353, LEU398, PRO400, ILE403, LEU404
(b) Bulnesol (90785)	−8.013	−8.013	−47.856	LEU257 (1.90)	SER347, THR354	LEU257, VA258, VAL259, ILE264, LEU287, ALA301, ALA302, ILE353, LEU398, ILE403, LEU404
(c) Champacol (227829)	−7.645	−7.645	−47.716	Not found	ASN261, THR262, SER347, THR354	LEU257, VA258, VAL259, ILE264, PRO281, LEU287, ALA301, ALA302, ALA346, ILE353, LEU404
4URO (antibacterial)						
(A) Co-crystallized ligand-4URO (antibacterial)	−5.809	−5.904	−62.448	ASN54 (2.12), GLU58 (2.35), ASP81 (2.08), GLY85 (2.53), GLN91 (1.97)	ASN54, SER55, GLN91, THR173	ILE51, VAL79, ILE86, PRO87, ALA98, VAL101, ILE102, ILE175
(B) Bulnesol (90785)	−5.771	−5.771	−40.741	GLU58 (1.59)	ASN54, SER55, SER128, THR173	ALA61, ILE86, ILE102, ILE175
(C) Champacol (227829)	−5.492	−5.492	−39.316	GLU58 (1.70)	ASN54, SER55, SER128, THR173	ILE86, ILE102, ILE175

ILE175. The polar amino acid residues are ASN54, SER55, GLN91, and THR173. Bulnesol (Figure 7) displayed a glide score of −5.771 kcal/mol, engaging in hydrogen bonding interactions with amino acid GLU58 at a relative distance of 1.59 Å. The hydrophobic interactions are seen with ALA61, ILE86, ILE102, and ILE175. The polar amino acid residues are ASN54, SER55, SER128, and THR173.

Figure 8 is the pictorial display of champacol interaction with the antibacterial target protein. It shows a glide score of −5.492 kcal/mol, and hydrogen bonding is evident with GLU58 at a distance of 1.70 Å. ILE86, ILE102, and ILE175 are hydrophobically engaged amino acids. The polar amino acid residues are ASN54, SER55, SER128, and THR173.

3.7 *In silico* ADME study

SwissADME is a web-based tool that uses computational models to predict ADME features of constituents based on their molecular structures. Table 8 highlights the predicted ADME properties and their compliance with Lipinski's rule of five. Most of the compounds investigated in the current study showed good gastrointestinal absorption and were compliant with Lipinski's rule of five, possessing not more than one hydrogen bond donor and one hydrogen bond acceptor. To sum up, the subsequent analysis of ADME properties and drug-likeness factors provide precious information about the potential of compounds to be developed as drugs, which can contribute to future drug design and drug development.

In silico predictions allow us to determine the theoretical biological parameters of bioactive constituents of plants under investigation. For bioactive molecules, it is mandatory to reach the body's target site, be bioavailable, and remain bioactive to initiate the targeted therapeutic effects. Therefore, the determination of ADME is highly in demand at an early stage of drug design and development [83]. *In vivo* studies are costly and time-consuming in drug development. Hence, in the drug development process, drug-likeness studies should be executed as early as possible with a view to save time and cost [84]. The structure or smiles of the compounds (ligands) are required to determine drug-likeness properties. We have evaluated the physicochemical parameters, such as lipid solubility (Log *P*), MW, water solubility (Log *S*), the topological surface area (TPSA, number of hydrogen bond donors (nHBD), rotatable bonds (RBs), and the number of hydrogen bond acceptors (nHBA). The molecular weight (MW) of all the derivatives is less than 500 Da, and the log *P* values of all the derivatives are less than 5, convincing that they have better

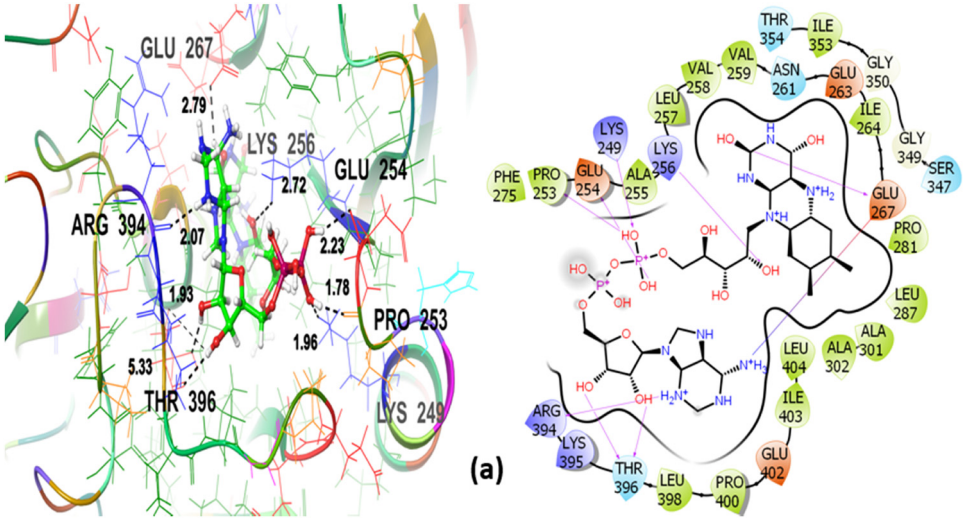

Figure 3: 3D and 2D interactive view of the crystallized ligand (a) with an anti-oxidant target protein (3NRZ).

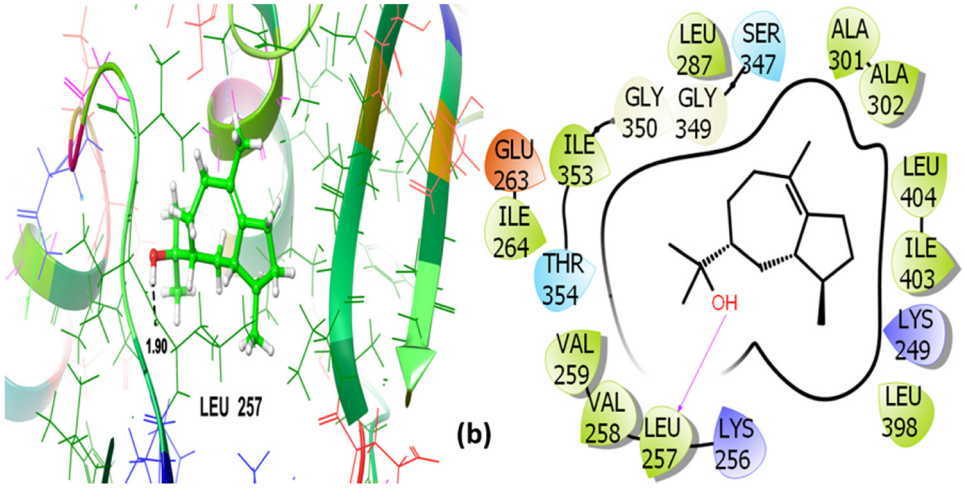

Figure 4: 3D and 2D interactive view of bulnesol (B) with an anti-oxidant target protein (3NRZ).

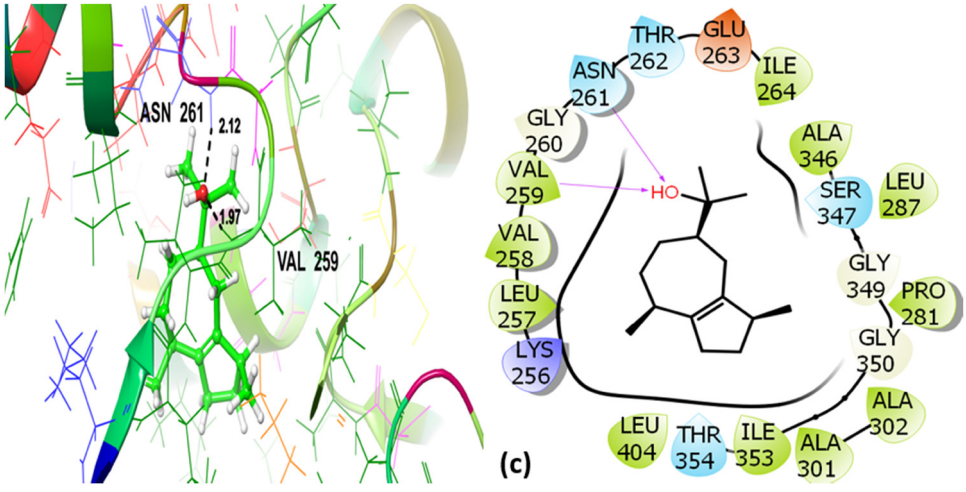

Figure 5: 3D and 2D interactive view of champacol (c) with an anti-oxidant target protein (3NRZ).

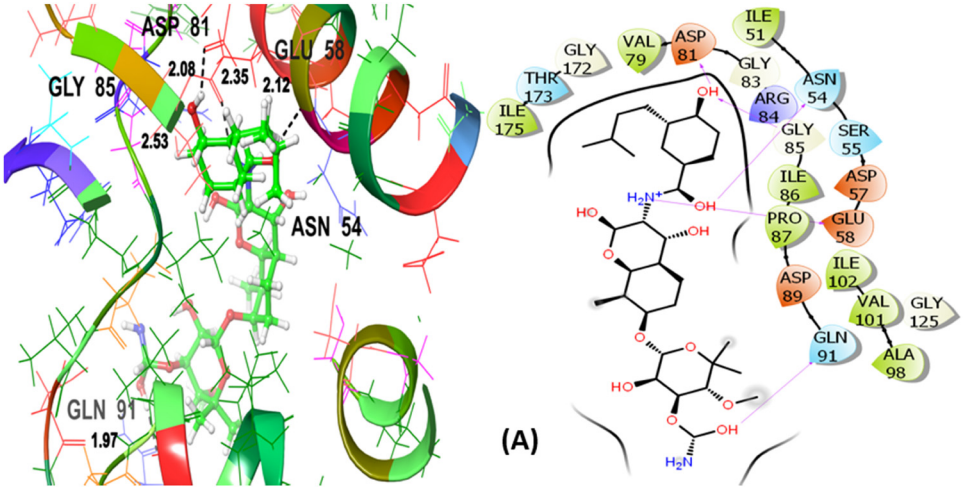

Figure 6: 3D and 2D interactive view of the co-crystallized ligand (A) with an antibacterial target protein (4URO).

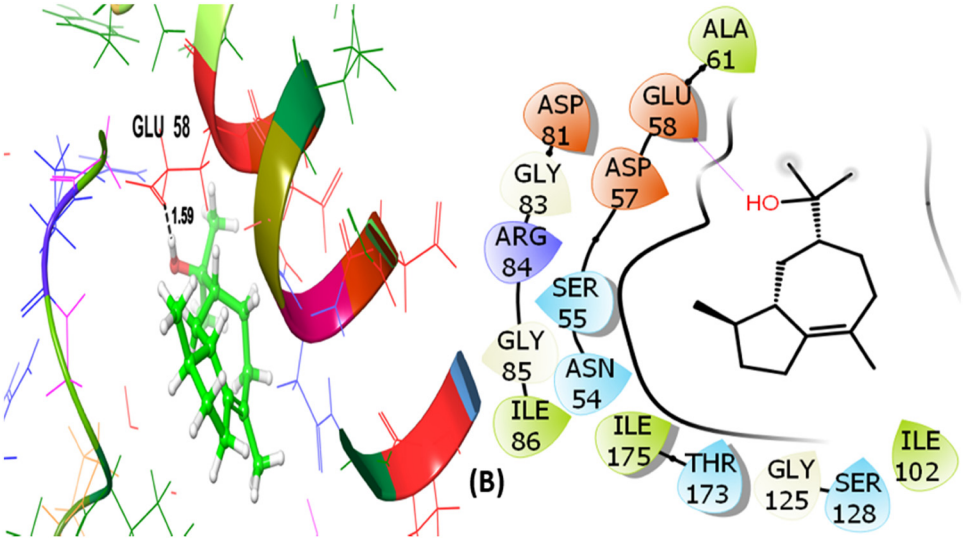

Figure 7: 3D and 2D interactive view of bulnesol (b) with an antibacterial target protein (4URO).

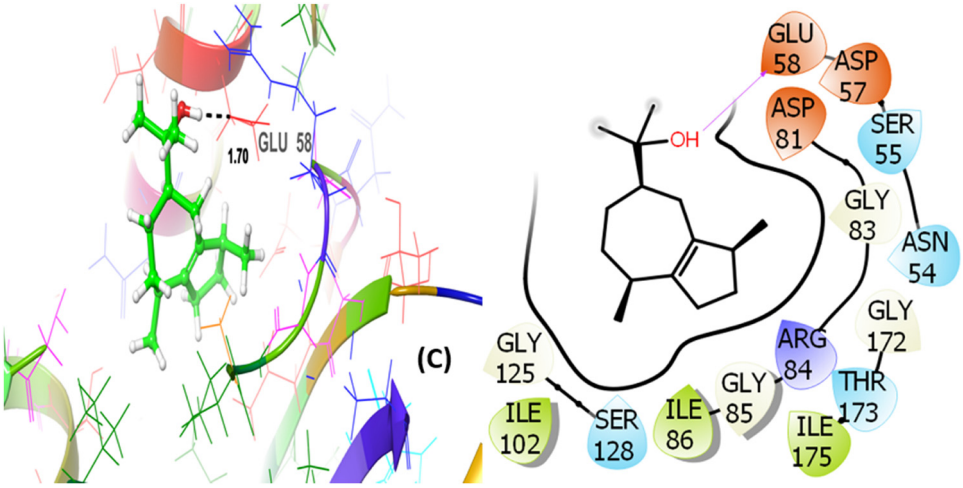

Figure 8: 3D and 2D interactive view of champacol (c) with an antibacterial target protein (4URO).

Table 8: ADME data of investigated ligands; the ADME parameters were evaluated using the online program SwissADME

Molecule	Canonical SMILES	MW	#Rotatable bonds	#H-bond acceptors	#H-bond donors	TPSA	Consensus Log *P*	Silicos-IT Log *Sw*	GI absorption	BBB permeant
2758	C[C@]12CC[C@H](CC1)C(O2)(C)C	154.25	0	1	0	9.23	2.67	−2.45	High	Yes
6654	CC1=CC[C@H]2C[C@@H]1C2(C)C	136.23	0	0	0	0	3.44	−2.23	Low	Yes
14896	C=C1CC[C@H]2C[C@@H]1C2(C)C	136.23	0	0	0	0	3.42	−2.48	Low	Yes
17100	CC1=CC[C@H](CC1)C(O)(C)C	154.25	1	1	1	20.23	2.49	−1.69	High	Yes
28237	C=C1CCC[C@@]2([C@@H]1C[C@H](CC2)C(=C)C)C	204.35	1	0	0	0	4.5	−3.8	Low	No
31253	C=CC(=C)CCC=C(C)C	136.23	4	0	0	0	3.43	−2.42	Low	Yes
90785	C[C@@H]1CCC2=C(C)CC[C@H](C[C@@H]12)C(O)(C)C	222.37	1	1	1	20.23	3.41	−2.96	High	Yes
90805	C[C@@H]1CC[C@@H]2C1=C[C@H](CC[C@H]2C)C(=C)C	204.35	1	0	0	0	4.31	−3.1	Low	No
91354	C[C@@H]1CC[C@@H]2[C@@H]1[C@H]1[C@H](C1(C)C)CCC2=C	204.35	0	0	0	0	4.34	−3.32	Low	Yes
91457	C=C1CCC[C@]2([C@H]1C[C@@H](CC2)C(O)(C)C)C	222.37	1	1	1	20.23	3.6	−3.21	High	Yes
94275	CC(=C)[C@@H]1CCC(=C2[C@@H](C1)[C@@H](C)CC2)C	204.35	1	0	0	0	4.3	−3.55	Low	No
227829	C[C@H]1CC[C@H](CC2=C1CC[C@@H]2C)C(O)(C)C	222.37	1	1	1	20.23	3.42	−2.96	High	Yes
440917	CC1=CC[C@@H](CC1)C(=C)C	136.23	1	0	0	0	3.37	−2.26	Low	Yes
1549992	CC(=CCC[C@]([C@@H]1CCC(=CC1)C)(O)C)C	222.37	4	1	1	20.23	3.76	−3	High	Yes
1742210	C=C1CC[C@H]2O[C@@]2(CC[C@@H]2[C@@H]1CC2(C)C)C	220.35	0	1	0	12.53	3.68	−3.51	High	Yes
5281515	C/C/1=C\CCC(=C)[C@@H]2[C@@H](CC1)C(C2)(C)C	204.35	0	0	0	0	4.24	−3.77	Low	No
5281516	C=C/C(=C/C/C=C(/CCC=C(C)C)\C)/C	204.35	6	0	0	0	4.96	−3.37	Low	No
5281517	C=CC(=C)CC/C=C(/CCC=C(C)C)\C	204.35	7	0	0	0	4.97	−3.74	Low	No
5281520	C/C/1=C\CC(C)(C)/C=C/C/C(=C/CC1)/C	204.35	0	0	0	0	4.26	−3.52	Low	No
5281522	C/C/1=C/CCC(=C)[C@@H]2[C@@H](CC1)C(C2)(C)C	204.35	0	0	0	0	4.24	−3.77	Low	No
5284507	C=C[C@@](CC/C=C(/CCC=C(C)C)\C)(O)C	222.37	7	1	1	20.23	4.19	−3.15	High	Yes
5315468	CC(=CC/C=C(/[C@H]1CCC(=CC1)C)\C)C	204.35	3	0	0	0	4.75	−3.21	Low	No
5317844	CC(=C)[C@@H]1CC[C@@H](C2=C(C1)[C@@H](C)CC2)C	204.35	1	0	0	0	4.3	−3.55	Low	No
5320250	C=C/C(=C\CC=C(C)C)/C	136.23	3	0	0	0	3.42	−2.04	Low	Yes
6429301	C/C/1=C\CCC(=C)[C@@H]2[C@H](CC1)C(C2)(C)C	204.35	0	0	0	0	4.23	−3.77	Low	No
6429302	CC(=CCC[C@]1(C)[C@H]2CC=C([C@@H]1C2)C)C	204.35	3	0	0	0	4.73	−3.55	Low	No
6432005	CC1=C2C[C@@H](CC[C@]2(CCC1)C)C(O)(C)C	222.37	1	1	1	20.23	3.6	−3.41	High	Yes
6432648	CC1=CCC[C@]2([C@H]1CC(=C(C)C)CC2)C	204.35	0	0	0	0	4.3	−3.75	Low	No
10104370	CC(=CCCC(=C)[C@H]1CCC(=CC1)C)C	204.35	4	0	0	0	4.83	−3.58	Low	No
91749531	C/C/1=C\CC(C)(C)/C=C\C[C@@]2([C@@H](CC1)O2)C	220.35	0	1	0	12.53				
101596917	CC1=C2[C@H]3[C@H](C3(C)C)CC[C@@]2(CCC1)C	204.35	0	0	0	0	4.43	−3.97	Low	No

membrane penetration and better antibacterial potential. The Log *S* values of all the derivatives are less than 0 to −5, which is also within the limit. The TPSA values of all the derivatives are less than 140 Å and have easy membrane penetration [85]. The more the negative value of Log *kp*, the higher the skin permeability. All the SCPZ SBs have Log *kp* values between −1.69 and −3.97. RB, nHBD, and nHBA are also key parameters for new drug candidates. It was estimated that all the investigated ligands have RB, nHBD, and nHBA values within the limit of Lipinski's rule of five.

Intestinal absorption is a key parameter in discovering orally biodegradable drugs [86]. In the intestine, the drug candidate should have significant absorption. A range of these ligands has high intestinal absorption and no blood–brain penetration and so fewer central nervous system side effects due to no blood–brain barrier penetration. It is concluded from the results in Table 3 that these bioactive constituents can be suitable drug candidates because they follow all the parameters of new drug candidates.

4 Conclusions

The current research aims to investigate the chemical composition, biological activities, and acute toxicity of CSEO. Chemical analyses revealed the dominance of sesquiterpenes, specifically β-caryophyllene (31.54%) and α-humulene (12.62%). Examination of the biological effects emphasized that CSEO exhibited anti-oxidant, antibacterial, and antifungal activities. Furthermore, toxicological studies have confirmed the EO's safety in terms of acute toxicity. Conclusively, this study adds to the developing body of literature that showcases the anti-oxidant and anti-microbial activities of CSEO. Additional experiments are necessary to pinpoint the primary components within the CSEO that contribute to its biological effects. This entails evaluating their synergistic effects to gain a better understanding of their combined action and their mechanism of action. Moreover, there is a necessity for further investigations into the toxicity of long-term exposure. The docking results emphasize the existence of a variety of molecular interactions that play a pivotal role in the binding affinities of the investigated ligands with their respective receptors. These interactions include hydrogen bonding, hydrophobic interactions, and polar contacts. The variations in binding scores and interaction patterns present valuable insights for fruitful comprehension of the potential effectiveness and specificity of these studied ligands as potential drugs or inhibitors in connection to the receptors under investigation. Most of the investigated bioactive constituents have good pharmacokinetic and pharmacodynamic parameters. Hence, these derivatives may be the better pharmacophore in exploring new bioactive moieties to treat diseases due to microbes and oxidative stress.

Acknowledgement: The authors extend their appreciation to the Researchers Supporting Project number (RSP2024R457), King Saud University, Riyadh, Saudi Arabia.

Funding information: This research was financially supported by the Researchers Supporting Project (number RSP2024R457), King Saud University, Riyadh, Saudi Arabia.

Author contributions: Conceptualization, original draft writing, reviewing, and editing: Rafik El-Mernissi, Naoual El Menyiy, Rania Moubachir, and Aziz Zouhri. Formal analysis, investigations, funding acquisition, reviewing, and editing: Yahya El-Mernissi, Farhan Siddique, Sumaira Nadeem, Hind Ibork, and Azeddin El Barnossi. Resources, data validation, data curation, and supervision: Gezahign Fentahun Wondmie, Mohammed Bourhia, Yousef A. Bin Jardan, Oualid Abboussi, and Lhoussain Hajji.

Conflict of interest: There is no conflict of interest.

Ethical approval: The conducted research is not related to either human or animal use.

Data availability statement: Data will be available upon request from the corresponding author.

References

[1] Eltayeb SAI, Ibrahim DAAM. Freeze drying. World J Pharm Res. 2015;4(6):96–111.

[2] Eid AM, Hawash M, Abualhasan M, Naser S, Dwaikat M, Mansour M. Exploring the potent anticancer, anti-microbial, and antiinflammatory effects of Capparis spinosa Oil Nanoemulgel. Coatings. 2023;13:1441.

[3] Zuardi AW. History of cannabis as a medicine: A review. Rev Bras Psiquiatr. 2006;28(2):153–7.

[4] Bonini SA, Premoli M, Tambaro S, Kumar A, Maccarinelli G, Memo M, et al. *Cannabis sativa*: A comprehensive ethnopharmacological review of a medicinal plant with a long history. J Ethnopharmacol. 2018 Dec;227:300–15. https://linkinghub.elsevier.com/retrieve/pii/S0378874118316611.

[5] Bachir F, Eddouks M, Arahou M, Fekhaoui M. Origin, early history, cultivation, and characteristics of the traditional varieties of Moroccan *Cannabis sativa* L. Cannabis Cannabinoid Res. 2022;7(5):603–15.

[6] ElSohly MA, Radwan MM, Gul W, Chandra S, Galal A. Phytochemistry of *Cannabis sativa* L. Progress in the chemistry of organic natural products. Vol. 103. Cham: Springer; 2017 p. 1–36. [cited 2023 Dec 6]. https://link.springer.com/chapter/10.1007/978-3-319-45541-9_1.

[7] Izzo AA, Borrelli F, Capasso R, Di Marzo V, Mechoulam R. Non-psychotropic plant cannabinoids: New therapeutic opportunities from an ancient herb. Trends Pharmacol. Sci. 2009;30:515–27.

[8] Amin MR, Ali DW. Pharmacology of medical Cannabis. In: Bukiya A, editor. Recent advances in cannabinoid physiology and pathology. Advances in experimental medicine and biology. Vol. 1162. Cham: Springer; 2019.

[9] Mechoulam R. Plant cannabinoids: A neglected pharmacological treasure trove. Br J Pharmacol. 2005;146:913–5. doi: 10.1038/sj.bjp.0706415.

[10] Hawash M, Jaradat N, Salhi NA, Shatreet B, Asbah AA, Hawash YH. Assessing the therapeutic potential and safety of traditional anti-obesity herbal blends in Palestine. Sci Rep. 2024;14(1):1–10. doi: 10.1038/s41598-024-52172-7

[11] Siddique S, Parveen Z, Firdaus-e-Bareen FB, Mazhar S. Chemical composition, antibacterial and anti-oxidant activities of essential oils from leaves of three Melaleuca species of Pakistani flora. Arab J Chem. 2020;13(1):67–74.

[12] Buckner MMC, Ciusa ML, Piddock LJV. Strategies to combat antimicrobial resistance: Anti-plasmid and plasmid curing. FEMS Microbiol Rev. Oxford Academic 2018;42:781–804. [cited 2024 Jan 31]. doi: 10.1093/femsre/fuy031

[13] Soriano A, Stefani S, Pletz MW, Menichetti F. Anti-microbial stewardship in patients with acute bacterial skin and skin-structure infections: An international Delphi consensus. J Glob Antimicrob Resist. 2020;22:296–301.

[14] Shaaban HAE, El-Ghorab AH, Shibamoto T. Bioactivity of essential oils and their volatile aroma components: Review. J Essent Oil Res. 2012 Apr;24(2):203–12. http://www.tandfonline.com/doi/abs/10.1080/10412905.2012.659528.

[15] Gutierrez J, Barry-Ryan C, Bourke P. Anti-microbial activity of plant essential oils using food model media: Efficacy, synergistic potential and interactions with food components. Food Microbiol. 2009;26(2):142–50. doi: 10.1016/j.fm.2008.10.008.

[16] Booth JK, Page JE, Bohlmann J. Terpene synthases from *Cannabis sativa*. Hamberger B, editor. PLoS One. 2017 Mar 29;12(3):e0173911, https://dx.plos.org/10.1371/journal.pone.0173911.

[17] Wanas AS, Radwan MM, Chandra S, Lata H, Mehmedic Z, Ali A, et al. Chemical composition of volatile oils of fresh and air-dried buds of Cannabis c hemovars, their insecticidal and repellent activities. Nat Prod Commun. 2020 May 19;15(5):1934578X2092672. http://journals.sagepub.com/doi/10.1177/1934578X20926729.

[18] Nissen L, Zatta A, Stefanini I, Grandi S, Sgorbati B, Biavati B, et al. Characterization and anti-microbial activity of essential oils of industrial hemp varieties (*Cannabis sativa* L.). Fitoterapia. 2010 Jul;81(5):413–9. https://linkinghub.elsevier.com/retrieve/pii/S0367326X09002780.

[19] El Bakali I, Sakar EH, Boutahar A, Kadiri M, Merzouki A. A comparative phytochemical profiling of essential oils isolated from three hemp (*Cannabis sativa* L.) cultivars grown in central-northern Morocco. Biocatal Agric Biotechnol. 2022;42:102327.

[20] Hawash M, Jaradat N, Abualhasan M, Thaher M, Sawalhi R, Younes N, et al. In vitro and in vivo assessment of the anti-oxidant potential of isoxazole derivatives. Sci Rep. 2022;12(1):1–8. doi: 10.1038/s41598-022-23050-x.

[21] Çapan İ, Hawash M, Jaradat N, Sert Y, Servi R, Koca İ. Design, synthesis, molecular docking and biological evaluation of new carbazole derivatives as anticancer, and anti-oxidant agents. BMC Chem. 2023;17(1):1–17.

[22] El Menyiy N, Bakour M, El Ghouizi A, El Guendouz S, Lyoussi B. Influence of geographic origin and plant source on physicochemical properties, mineral content, and anti-oxidant and antibacterial activities of Moroccan propolis. Int J Food Sci. 2021;2021:1–12.

[23] Zouhri A, Bouddine T, Menyiy NEl, Kachkoul R, El-mernissi Y, Siddique F, et al. Ionomic analysis, polyphenols characterization, analgesic, antiinflammatory and anti-oxidant capacities of Cistus laurifolius leaves: in vitro, in vivo, and in silico investigations. Sci Rep. 2023;13(1):1–18. doi: 10.1038/s41598-023-50031-5

[24] Balouiri M, Sadiki M, Ibnsouda SK. Methods for in vitro evaluating anti-microbial activity: A review. J Pharm Anal. 2016;6:71–9.

[25] El Barnossi A, Moussaid F, Iraqi Housseini A. Antifungal activity of Bacillussp. Gn-A11-18isolated from decomposing solid green household waste in water and soil against Candida albicans and Aspergillus niger. In: Akhssas A, Baba K, Bahi L, Benradi F, Cherkaoui E, Khamar M, et al., editors. E3S Web Conf. 150, 2020 Feb 12. 02003. https://www.e3s-conferences.org/10.1051/e3sconf/202015002003.

[26] Pereira E, Santos A, Reis F, Tavares RM, Baptista P, Lino-Neto T, et al. A new effective assay to detect anti-microbial activity of filamentous fungi. Microbiol Res. 2013;168:1–5.

[27] Elegbede JA, Lateef A, Azeez MA, Asafa TB, Yekeen TA, Oladipo IC, et al. Silver-gold alloy nanoparticles biofabricated by fungal xylanases exhibited potent biomedical and catalytic activities. Biotechnol Prog. 2019;35:1–13. doi: 10.1002/btpr.2829.

[28] Sarker SD, Nahar L, Kumarasamy Y. Microtitre plate-based antibacterial assay incorporating resazurin as an indicator of cell growth, and its application in the in vitro antibacterial screening of phytochemicals. Methods. 2007;42(4):321–4. doi: 10.1016/j.ymeth.2007.01.006.

[29] Agour A, Mssillou I, Mechchate H, Es-Safi I, Allali A, El Barnossi A, et al. Brocchia cinerea (Delile) Vis. essential oil anti-microbial activity and crop protection against cowpea weevil Callosobruchus maculatus (Fab.). Plants. 2022;11(5):1–13.

[30] Test No. 423: Acute Oral toxicity - Acute Toxic Class Method [Internet]. Test. OECD; 2002. p. 1–11. (OECD Guidelines for the Testing of Chemicals, Section 4; Vol. 1986). https://www.oecd-ilibrary.org/environment/test-no-423-acute-oral-toxicity-acute-toxic-class-method_9789264071001-en.

[31] Aarthi S, Keerthana T, Puniethaa P. 3D pharamacophore model, virtual screening, binding affinity and molecular dynamics studies of potential anticancerous compounds against mammalian target rapamycin. 2023 Jul. doi: 10.21203/rs.3.rs-3100361/v1.

[32] Berman HM. The protein data bank. Nucleic Acids Res. 2000 Jan;28(1):235–42.

[33] Di Sotto A, Gullì M, Acquaviva A, Tacchini M, Di Simone SC, Chiavaroli A, et al. Phytochemical and pharmacological profiles of the essential oil from the inflorescences of the *Cannabis sativa* L. Ind Crop Products. 2022;183:114980.

[34] Gulluni N, Re T, Loiacono I, Lanzo G, Gori L, Macchi C, et al. Cannabis essential oil: A preliminary study for the evaluation of the brain effects. Evid-Based Complement Altern Med. 2018;2018:1–11. https://www.hindawi.com/journals/ecam/2018/1709182/.

[35] Benelli G, Pavela R, Petrelli R, Cappellacci L, Santini G, Fiorini D, et al. The essential oil from industrial hemp (*Cannabis sativa* L.) by-

products as an effective tool for insect pest management in organic crops. Ind Crop Prod. 2018 Oct;122:308–15. https://linkinghub.elsevier.com/retrieve/pii/S0926669018304515.

[36] Palmieri S, Maggio F, Pellegrini M, Ricci A, Serio A, Paparella A, et al. Effect of the distillation time on the chemical composition, anti-oxidant potential and anti-microbial activity of essential oils from different *Cannabis sativa* L. Cultivars. Molecules. 2021;26:4770.

[37] Judžentienė A, Garjonytė R, Būdienė J. Phytochemical composition and anti-oxidant activity of various extracts of fibre hemp (*Cannabis sativa* L.) cultivated in Lithuania. Molecules. 2023;28(13):4928.

[38] Vuerich M, Ferfuia C, Zuliani F, Piani B, Sepulcri A, Baldini M. Yield and quality of essential oils in hemp varieties in different environments. Agronomy. 2019;9:356.

[39] Fiorini D, Molle A, Nabissi M, Santini G, Benelli G, Maggi F. Valorizing industrial hemp (*Cannabis sativa* L.) by-products: Cannabidiol enrichment in the inflorescence essential oil optimizing sample pre-treatment prior to distillation. Ind Crop Prod. 2019 Feb;128:581–9. https://linkinghub.elsevier.com/retrieve/pii/S092666901830918X.

[40] Menghini L, Ferrante C, Carradori S, D'antonio M, Orlando G, Cairone F, et al. Chemical and bioinformatics analyses of the anti-leishmanial and anti-oxidant activities of hemp essential oil. Biomolecules. 2021;11:1–17.

[41] Zengin G, Menghini L, Di Sotto A, Mancinelli R, Sisto F, Carradori S, et al. Chromatographic analyses, in vitro biological activities, and cytotoxicity of *Cannabis sativa* L. essential oil: A multidisciplinary study. Molecules. 2018 Dec;23(12):3266. http://www.mdpi.com/1420-3049/23/12/3266.

[42] Pieracci Y, Ascrizzi R, Terreni V, Pistelli L, Flamini G, Bassolino L, et al. Essential oil of *cannabis sativa* l: Comparison of yield and chemical composition of 11 hemp genotypes. Molecules. 2021;26:4080.

[43] Rodríguez BC, Durán-Zuazo VH, García-Tejero IF, Ruiz BG. Current and future applications for hemp essential oils: a review. In Current applications, approaches and potential perspectives for hemp: Crop management, industrial usages, and functional purposes. Elsevier; 2022. p. 365–91.

[44] Nafis A, Kasrati A, Jamali CA, Mezrioui N, Setzer W, Abbad A, et al. Anti-oxidant activity and evidence for synergism of *Cannabis sativa (L.*)essential oil with anti-microbial standards. Ind Crop Products. 2019;137:396–400.

[45] Abd-ElGawad A, El Gendy AEN, El-Amier Y, Gaara A, Omer E, Al-Rowaily S, et al. Essential oil of Bassia muricata: Chemical characterization, anti-oxidant activity, and allelopathic effect on the weed Chenopodium murale. Saudi J Biol Sci. 2020 Jul;27(7):1900–6. https://linkinghub.elsevier.com/retrieve/pii/S1319562X20301303.

[46] Novak J, Zitterl-Eglseer K, Deans SG, Franz CM. Essential oils of different cultivars of *Cannabis sativa* L. and their anti-microbial activity. Flavour Fragr J. 2001 Jul;16(4):259–62. https://onlinelibrary.wiley.com/doi/10.1002/ffj.993.

[47] Kumeroa F, Komahan S, Sofkova-Bobcheva S, Clavijo McCormick A. Characterization of the volatile profiles of six industrial hemp (*Cannabis sativa* L.) cultivars. Agronomy. 2022;12:2651.

[48] Elhidar N, Nafis A, Kasrati A, Goehler A, Bohnert JA, Abbad A, et al. Chemical composition, anti-microbial activities and synergistic effects of essential oil from Senecio anteuphorbium, a Moroccan endemic plant. Ind Crop Prod. 2019;130(January):310–5.

[49] Laaroussi H, Ferreira-Santos P, Genisheva Z, Bakour M, Ousaaid D, Teixeira JA, et al. Unraveling the chemical composition, anti-oxidant, α-amylase and α-glucosidase inhibition of Moroccan propolis. Food Biosci. 2021 Aug;42(May):101160. https://linkinghub.elsevier.com/retrieve/pii/S2212429221002856.

[50] Gushiken LFS, Beserra FP, Hussni MF, Gonzaga MT, Ribeiro VP, De Souza PF, et al. Beta-caryophyllene as an anti-oxidant, antiinflammatory and re-epithelialization activities in a rat skin wound excision model. Oxid Med Cell Longev. 2022;2022:1–21.

[51] Ruberto G, Baratta MT. Anti-oxidant activity of selected essential oil components in two lipid model systems. Food Chem. 2000 May;69(2):167–74. https://linkinghub.elsevier.com/retrieve/pii/S0308814699002472.

[52] Bonamin F, Moraes TM, dos Santos RC, Kushima H, Faria FM, Silva MA, et al. The effect of a minor constituent of essential oil from Citrus aurantium: The role of β-myrcene in preventing peptic ulcer disease. Chem Biol Interact. 2014 Apr;212:11–9. https://linkinghub.elsevier.com/retrieve/pii/S0009279714000179.

[53] Xanthis V, Fitsiou E, Voulgaridou GP, Bogadakis A, Chlichlia K, Galanis A, et al. Anti-oxidant and cytoprotective potential of the essential oil Pistacia lentiscus var. chia and its major components myrcene and α-pinene. Anti-oxidants. 2021 Jan 18;10(1):127. https://www.mdpi.com/2076-3921/10/1/127.

[54] Palmieri S, Maggio F, Pellegrini M, Ricci A, Serio A, Paparella A, et al. Effect of the distillation time on the chemical composition, anti-oxidant potential and anti-microbial activity of essential oils from different *Cannabis sativa* L. cultivars. Molecules. 2021 Aug 6;26(16):4770. https://www.mdpi.com/1420-3049/26/16/4770.

[55] Pellegrini M, Palmieri S, Ricci A, Serio A, Paparella A, Lo Sterzo C. In vitro anti-oxidant and anti-microbial activity of *Cannabis sativa* L. cv 'Futura 75' essential oil. Nat Prod Res. 2021 Dec 17;35(24):6020–4. https://www.tandfonline.com/doi/full/10.1080/14786419.2020.1813139.

[56] Wanas AS, Radwan MM, Mehmedic Z, Jacob M, Khan IA, Elsohly MA. Antifungal activity of the volatiles of high potency *Cannabis sativa L.* Against Cryptococcus neoformans. Rec Nat Products. 2015;10:214–20.

[57] Zheljazkov VD, Sikora V, Semerdjieva IB, Kačániová M, Astatkie T, Dincheva I. Grinding and fractionation during distillation alter hemp essential oil profile and its anti-microbial activity. Molecules. 2020 Aug 28;25(17):3943. https://www.mdpi.com/1420-3049/25/17/3943.

[58] Zheljazkov VD, Sikora V, Dincheva I, Kačániová M, Astatkie T, Semerdjieva IB, et al. Industrial, CBD, and wild hemp: How different are their essential oil profile and anti-microbial activity? Molecules. 2020 Oct 12;25(20):4631. https://www.mdpi.com/1420-3049/25/20/4631.

[59] Iseppi R, Brighenti V, Licata M, Lambertini A, Sabia C, Messi P, et al. Chemical characterization and evaluation of the antibacterial activity of essential oils from fibre-type *Cannabis sativa L.* (Hemp). Molecules. 2019 Jun 21;24(12):2302. https://www.mdpi.com/1420-3049/24/12/2302.

[60] Bouyahya A, Bakri Y, Et-Touys A, Talbaoui A, Khouchlaa A, Charfi S, et al. Résistance aux antibiotiques et mécanismes d'action des huiles essentielles contre les bactéries. Phytothérapie. 2017 Mar 15;22(6):567–70. https://www.sciencedirect.com/science/article/abs/pii/S0992594521001082.

[61] Dahham S, Tabana Y, Iqbal M, Ahamed M, Ezzat M, Majid A, et al. The anticancer, anti-oxidant and anti-microbial properties of the sesquiterpene β-caryophyllene from the essential oil of Aquilaria crassna. Molecules. 2015 Jun 26;20(7):11808–29. http://www.mdpi.com/1420-3049/20/7/11808.

[62] Francomano F, Caruso A, Barbarossa A, Fazio A, La Torre C, Ceramella J, et al. β-caryophyllene: A sesquiterpene with countless biological properties. Appl Sci (Switz). 2019;9:5420. https://www.mdpi.com/2076-3417/9/24/5420.
[63] Schofs L, Sparo MD, Sánchez Bruni SF. The anti-microbial effect behind Cannabis sativa. Pharmacol Res Perspect. 2021;9:761–78.
[64] Dorman HJD, Deans SG. Anti-microbial agents from plants: Antibacterial activity of plant volatile oils. J Appl Microbiol. 2000;88:308–16.
[65] Połeć K, Broniatowski M, Wydro P, Hąc-Wydro K. The impact of β-myrcene – the main component of the hop essential oil – on the lipid films. J Mol Liq. 2020 Jun;308:113028. https://linkinghub.elsevier.com/retrieve/pii/S016773222031000X.
[66] Novak J, Zitterl-Eglseer K, Deans SG, Franz CM. Essential oils of different cultivars of *Cannabis sativa* L. And their anti-microbial activity. Flavour Fragr J. 2001 Jul;16(4):259–62. https://onlinelibrary.wiley.com/doi/10.1002/ffj.993.
[67] Tian J, Ban X, Zeng H, He J, Huang B, Wang Y. Chemical composition and antifungal activity of essential oil from Cicuta virosa L. var. latisecta Celak. Int J Food Microbiol. 2011;145:464–70.
[68] Hyldgaard M, Mygind T, Meyer RL. Essential oils in food preservation: Mode of action, synergies, and interactions with food matrix components. Front Microbiol. 2012;3(Jan):1–24.
[69] Jassal K, Kaushal S, Rashmi, Rani R. Antifungal potential of guava (Psidium guajava) leaves essential oil, major compounds: beta-caryophyllene and caryophyllene oxide. Arch Phytopathol Plant Prot. 2021 Dec 14;54(19–20):2034–50. [cited 2023 Nov 19]. https://www.tandfonline.com/doi/abs/10.1080/03235408.2021.1968287.
[70] Nazzaro F, Fratianni F, Coppola R, De Feo V. Essential oils and antifungal activity. Pharmaceuticals. 2017 Nov;10(4):86. http://www.mdpi.com/1424-8247/10/4/86.
[71] Cakir A, Kordali S, Zengin H, Izumi S, Hirata T. Composition and antifungal activity of essential oils isolated from Hypericum hyssopifolium and Hypericum heterophyllum. Flavour Fragr J. 2004 Jan 18;19(1):62–8. https://onlinelibrary.wiley.com/doi/10.1002/ffj.1279.
[72] Maccioni A, Falconieri D, Porcedda S, Piras A, Gonçalves MJ, Alves-Silva JM, et al. Antifungal activity and chemical composition of the essential oil from the aerial parts of two new Teucrium capitatum L. chemotypes from Sardinia Island, Italy. Nat Prod Res. 2021 Dec 17;35(24):6007–13. https://www.tandfonline.com/doi/full/10.1080/14786419.2020.1813136.
[73] Ali EMM, Almagboul AZI, Khogali SME, Gergeir UMA. Anti-microbial activity of *Cannabis sativa* L. Chin Med. 2012;3(March):61–4. https://www.mendeley.com/search/?page=1&query=Antimicrobial activity of Cannabis&sortBy=relevance.
[74] Orlando G, Adorisio S, Delfino D, Chiavaroli A, Brunetti L, Recinella L, et al. Comparative investigation of composition, antifungal, and antiinflammatory effects of the essential oil from three industrial hemp varieties from Italian cultivation. Antibiotics. 2021 Mar 22;10(3):334. https://www.mdpi.com/2079-6382/10/3/334.
[75] Vozza Berardo ME, Mendieta JR, Villamonte MD, Colman SL, Nercessian D. Antifungal and antibacterial activities of *Cannabis sativa* L. resins. J Ethnopharmacol. 2024 Jan;318:116839. https://linkinghub.elsevier.com/retrieve/pii/S0378874123007079.
[76] Adassi MB, Ngoupaye GT, Yassi FB, Foutsop AF, Kom TD, Ngo Bum E. Revealing the most effective anticonvulsant part of Malvaviscus arboreus Dill. Ex Cav. and its acute and sub-acute toxicity. J Ethnopharmacol. 2023 Mar;303:115995. https://linkinghub.elsevier.com/retrieve/pii/S0378874122010340.
[77] Mazzara E, Petrelli R, Torresi J, Ricciardi R, Benelli G, Maggi F. Hemp essential oil: an innovative product with potential industrial applications. In: Current applications, approaches and potential perspectives for hemp: Crop management, industrial usages, and functional purposes. Academic Press; 2022. p. 201–79.
[78] Balafrej T, Skalli S, Benaich S, Labyad A, Akoh R, El Mskini FZ, et al. Acute oral toxicity of *Cannabis sativa* L. co-products in mice. Not Sci Biol. 2023;15:11591.
[79] Pingale SS, Virkar PS, Mahale RG, Wirnkor VA. Toxicity study of coriandrum Sativum Linn. Int J Mod Pharm Res. 2021;5(2):42–8. www.ijmpronline.com.
[80] Yassa HA, Dawood AEWA, Shehata MM, Abdel-Hady RH, Abdel Aal KM. Subchronic toxicity of cannabis leaves on male albino rats. Hum Exp Toxicol. 2010;29(1):37–47.
[81] Bailey MM, Emily Mills MC, Haas AE, Bailey K, Kaufmann RC. The effects of subacute exposure to a water-soluble cannabinol compound in male mice. J Cannabis Res. 2022;4:44. doi: 10.1186/s42238-022-00153-w.
[82] Babson KA, Sottile J, Morabito D. Cannabis, cannabinoids, and sleep: A review of the literature. Curr Psychiatry Reports. 2017;19:23. http://link.springer.com/10.1007/s11920-017-0775-9.
[83] Jagadesh Babu K, Ayodhya D, Shivaraj. Comprehensive investigation of Co(II), Ni(II) and Cu(II) complexes derived from a novel Schiff base: Synthesis, characterization, DNA interactions, ADME profiling, molecular docking, and in-vitro biological evaluation. Results Chem. 2023 Dec;6:101110.
[84] Strzelecka M, Wiatrak B, Jawień P, Czyżnikowska Ż, Świątek P. New Schiff bases derived from dimethylpyridine-1,2,4-triazole hybrid as cytotoxic agents targeting gastrointestinal cancers: Design, synthesis, biological evaluation and molecular docking studies. Bioorg Chem. 2023 Oct;139:106758.
[85] Oladipo SD, Luckay RC, Olofinsan KA, Obakachi VA, Zamisa SJ, Adeleke AA, et al. Antidiabetes and anti-oxidant potential of Schiff bases derived from 2-naphthaldehye and substituted aromatic amines: Synthesis, crystal structure, Hirshfeld surface analysis, computational, and invitro studies. Heliyon. 2024 Jan;10(1):e23174.
[86] Sjögren E, Westergren J, Grant I, Hanisch G, Lindfors L, Lennernäs H, et al. In silico predictions of gastrointestinal drug absorption in pharmaceutical product development: Application of the mechanistic absorption model GI-Sim. Eur J Pharm Sci. 2013 Jul;49(4):679–98.